NAVAL POSTGRADUATE SCHOOL
MONTEREY, CALIFORNIA

THESIS

DEVELOPMENT AND ASSESSMENT
OF A SHIP
MANEUVERING SIMULATION MODEL

by

Patrick B. LaFontant
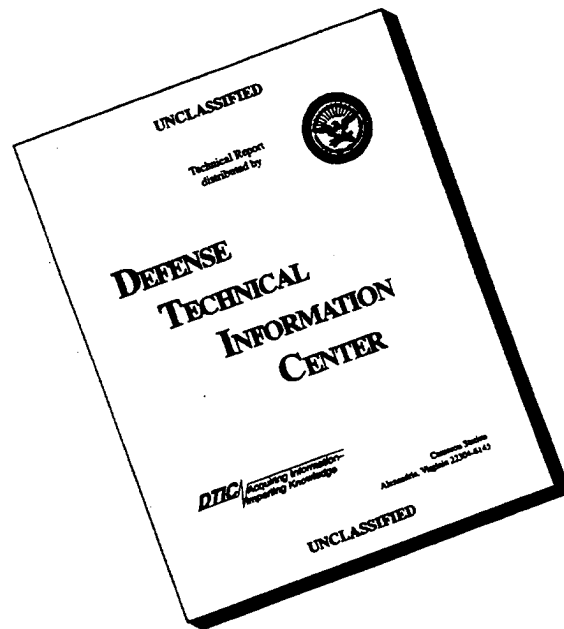
December, 1995

Thesis Advisor: Fotis Papoulias

Approved for public release; distribution is unlimited.

DISCLAIMER NOTICE

THIS DOCUMENT IS BEST
QUALITY AVAILABLE. THE
COPY FURNISHED TO DTIC
CONTAINED A SIGNIFICANT
NUMBER OF PAGES WHICH DO
NOT REPRODUCE LEGIBLY.

REPORT DOCUMENTATION PAGE

Form Approved OMB No. 0704-0188

1. AGENCY USE ONLY *(Leave blank)*	2. REPORT DATE December 1995	3. REPORT TYPE AND DATES COVERED Master's Thesis

4. TITLE AND SUBTITLE Development and Assessment of a Ship Maneuvering Simulation Model.	5. FUNDING NUMBERS
6. AUTHOR(S) Patrick B. LaFontant	

7. PERFORMING ORGANIZATION NAME(S) AND ADDRESS(ES) Naval Postgraduate School Monterey CA 93943-5000	8. PERFORMING ORGANIZATION REPORT NUMBER

9. SPONSORING/MONITORING AGENCY NAME(S) AND ADDRESS(ES)	10. SPONSORING/MONITORING AGENCY REPORT NUMBER

11. SUPPLEMENTARY NOTES The views expressed in this thesis are those of the author and do not reflect the official policy or position of the Department of Defense or the U.S. Government.

12a. DISTRIBUTION/AVAILABILITY STATEMENT Approved for public release; distribution is unlimited.	12b. DISTRIBUTION CODE

13. ABSTRACT *(maximum 200 words)*

A nonlinear maneuvering model based on ship geometric and mass properties is developed. The model can be utilized to evaluate maneuvering performance early in the design phase. This model is also used in this thesis as a benchmark in order to evaluate the accuracy of the simpler Nomoto's model. The latter is faster to simulate and is ideally suited for visual simulation studies. Results comparing the relative accuracy and speed of implementation of the two models are presented for different inputs and geometric properties. An improvement to Nomoto's model is suggested which greatly increases accuracy while maintaining high speed of real time implementation. Furthermore, a series of parametric studies is performed in order to evaluate the sensitivity of fundamental maneuvering properties in terms of basic ship geometric quantities.

14. SUBJECT TERMS Maneuvering Simulation Modeling	15. NUMBER OF PAGES 54
	16. PRICE CODE

17. SECURITY CLASSIFICATION OF REPORT Unclassified	18. SECURITY CLASSIFICATION OF THIS PAGE Unclassified	19. SECURITY CLASSIFICATION OF ABSTRACT Unclassified	20. LIMITATION OF ABSTRACT UL

NSN 7540-01-280-5500

Standard Form 298 (Rev. 2-89)
Prescribed by ANSI Std. 239-18 298-102

DEVELOPMENT AND ASSESSMENT
OF A SHIP
MANEUVERING SIMULATION MODEL

Patrick B. LaFontant
Lieutenant, United States Navy
B.S., Hampton University, 1989

Submitted in partial fulfillment
of the requirements for the degree of

MASTER OF SCIENCE IN MECHANICAL ENGINEERING

from the

NAVAL POSTGRADUATE SCHOOL
December 1995

Author: _____

Patrick B. LaFontant

Approved by: _____

Fotis Papoulias, Thesis Advisor

_____

Matthew Kelleher, Chairman
Department of Mechanical Engineering

ABSTRACT

A nonlinear maneuvering model based on ship geometric and mass properties is developed. The model can be utilized to evaluate maneuvering performance early in the design phase. This model is also used in this thesis as a benchmark in order to evaluate the accuracy of the simpler Nomoto's model. The latter is faster to simulate and is ideally suited for visual simulation studies. Results comparing the relative accuracy and speed of implementation of the two models are presented for different inputs and geometric properties. An improvement to Nomoto's model is suggested which greatly increases accuracy while maintaining high speed of real time implementation. Furthermore, a series of parametric studies is performed in order to evaluate the sensitivity of fundamental maneuvering properties in terms of basic ship geometric quantities.

TABLE OF CONTENTS

I. INTRODUCTION

Today's military faces many challenges to do more with less. Since the end of the Cold War, the topic of discussion on Capitol Hill has been the shrinking military budget. However, the military's requirement to maintain full combat readiness has not changed. In order to maintain training at the required level, alternatives to costly full scale maneuvers must be developed.

Current war gaming models use mostly static or simplified dynamic descriptions of both attacking weapons and targets. Clearly, this provides an unrealistic description of the situation, with respect to the vulnerability of the target to attack, and does not allow for the incorporation of standard tactical maneuvers of the target to avoid incoming weapons. What needs to be done is to increase the accuracy of current models by incorporation of targets in a dynamic, rather than a static manner. Developing an accurate simulation model, will lead to ship designers being able to examine the vulnerability of a ship, in real time through the simulation model.

In this thesis, a nonlinear model based on ship geometric and mass properties will be developed. The model can be utilized to evaluate maneuvering performance early in the design phase. This model will also serve as a benchmark in order to evaluate the relative accuracy of a simpler linear model. Chapter II will show the development of the mathematical models. Chapter III will discuss the assessment of the models and compare them for visual simulation suitability. Chapter IV will evaluate the sensitivity of fundamental maneuvering properties in terms of basic ship geometric quantities. Chapter V will assess two variations to the linear model, and compare them to the nonlinear model. Finally, Chapter VI will discuss conclusions and recommendations for further work.

II. MATHEMATICAL MODELING

In this dynamical model, the planar motion of a ship on an undisturbed free-surface of an incompressible fluid will be considered. The basic dynamics of maneuvering will be described and analyzed using Newton's equations of motion.

We will define two reference frames, one set of axes fixed relative to the Earth aligned with directions North, East, and Down (denoted by capital letters), and a second set of axes fixed relative to the ship, aligned with the longitudinal, the starboard direction, and down (denoted by lower case letters).
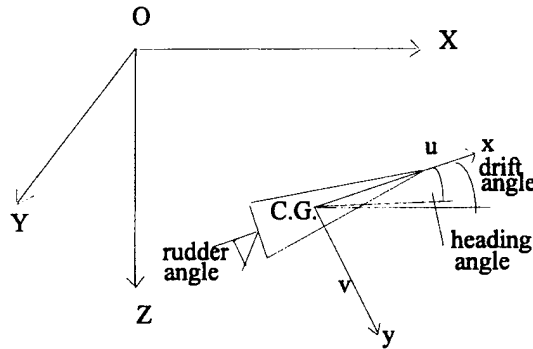
Figure 1 Designation of reference frames

The heading (yaw) angle, refers to the direction of the ship's longitudinal axis, with respect to one of the fixed axes. The drift angle refers to the difference between the heading and the actual course. Let the instantaneous speed of the ship be denoted by U, then the surge and sway velocities are given by:

$$u = U\cos\beta \quad , \quad v = -U\sin\beta$$

3

The dynamical model used in this work has been proposed [Ref. 1] and is given by:

$$X' - (m' + m_x')(L/U)(\dot{U}\cos\beta/U - \dot{\beta}\sin\beta) + (m' + m_y')r'\sin\beta$$

$$Y' - -(m' + m_y')(L/U)(\dot{U}\sin\beta/U + \dot{\beta}\cos\beta) + (m' + m_x')r'\cos\beta$$

$$N' - (I_{zz}' + i_{zz}')(L/U^2)(\dot{U}r' + U\dot{r}')$$

where,

β is the drift angle

r is the rotational or yaw velocity

I_{zz}, and i_{zz} are the mass moments of inertia in both ref frames

m, m_x, and m_y are the ship's mass, added mass of the x-axis, and the added mass of the y-axis, respectively

All terms of these equations, and the equations of motion in the remaining report, have been nondimensionalized using the ship's length L, the ship's draft d, the fluids density ρ, and the ship's speed U, as shown in the Appendix The terms X, Y, and N are the external force along the x-axis, the external force along the y-axis, and the yaw moment about the ship's center of gravity, respectively.

It is assumed that X, Y, and N have the following decomposition,

$$X - X_H + X_P + X_R$$

$$Y - Y_H + Y_P + Y_R$$

$$N - N_H + N_P + N_R$$

where the subscripts represent respective contribution due to,

H - ship's hull

4

P - ship's propeller

R - ship's rudder

We can assume that during most ordinary maneuvers, the forward velocity is kept constant by the propulsion control. Also, in looking at the ship's response to rudder deflection, it is assumed that no significant surge accelerations will take place. From these assumptions we are left with,

$$Y = Y_H + Y_R$$

$$N = N_H + N_R$$

The components of the rudder forces are taken to be of the form,

$$Y_R = -(1 + a_H) F_N \cos\delta$$

$$N_R = -(x_R + a_H x_H) F_N \cos\delta$$

$$F_N = -(A_R/Ld) C_N U_R^2 \sin(\delta - (\beta - 2x_R r))$$

$$C_N = 6.13 K_R/(K_R + 2.25)$$

where,

F_N - force acting on rudder

A_R - rudder area

K_R - rudder aspect ratio

U_R - effective rudder inflow speed (taken to be equal to U)

x_R - distance between COG of ship and center of lateral force

x_H - distance between COG of ship and center of additional lateral
force

a_H - ratio of additional lateral force

A_R, K_R, x_R, x_H, and a_H are constants obtained through model tests.

The lateral force and yaw moment acting on the ship's hull are expressed as follows:

$$Y_H = Y_\beta \beta + Y_r r + Y_{\beta\beta} \beta |\beta| + Y_{rr} r |r| + (Y_{\beta\beta r} \beta + Y_{\beta rr} r) \beta r$$

$$N_H = N_\beta \beta + N_r r + N_{\beta\beta} \beta |\beta| + N_{rr} r |r| + (N_{\beta\beta r} \beta + N_{\beta rr} r) \beta r$$

The lateral force and yaw moment hydrodynamic coefficients are given as,

$$Y_r = m_1 - 1.5 s C_B$$

$$Y_\beta = \frac{1}{2} \pi k + 1.4 s C_B$$

$$Y_{\beta rr} = 2.97 \frac{k}{s} (1 - C_B)$$

$$Y_{\beta\beta} = 1.25 \frac{k}{s} (1 - C_B) + 0.5$$

$$Y_{rr} = 0.17 \frac{k}{s} C_B - 0.07$$

$$Y_{\beta\beta r} = 0.75 \frac{k}{s} C_B - 0.65$$

$$N_r = -0.54 k + k^2$$

$$N_\beta = -k$$

$$N_{\beta\beta} = -0.48 \frac{k}{s} (1 - C_B) + 0.66$$

$$N_{rr} = 0.5 s C_B - 0.09$$

$$N_{\beta rr} = -0.25 \frac{k}{s} C_B + 0.05$$

$$N_{\beta\beta r} = -57.5 (s C_B)^2 + 18.4 s C_B - 1.6$$

where,

$$s = B/L, \quad Slenderness \ ratio$$

$$k = 2d/L, \quad Aspect \ ratio$$

$$C_B = \frac{V}{LdB}, \quad Block \ coefficient$$

$$m_1 = 2sC_B(1+k), \quad Mass \ coefficient$$

The above model may be simplified by linearizing the sway and yaw equations, as done in [Ref. 3], to obtain,

$$(m-Y_{\dot{v}})\dot{v} - (Y_{\dot{r}} - mx_G)\dot{r} = Y_v v + (Y_r - mU)r + Y_\delta \delta$$

$$(I_z - N_{\dot{r}})\dot{r} - (N_{\dot{v}} - mx_G)\dot{v} = N_v v + (N_r - mx_G U)r + N_\delta \delta$$

where δ is the rudder deflection angle measured according to the convention of Figure (1); positive rudder corresponds to a turn to port. These equations of motion can be manipulated to produce a pair of decoupled second order equations in r and v,

$$T_1 T_2 \ddot{r} + (T_1 + T_2)\dot{r} + r = K\delta + KT_3 \dot{\delta}$$

$$T_1 T_2 \ddot{v} + (T_1 + T_2)\dot{v} + v = K_v \delta + K_v T_4 \dot{\delta}$$

We will assume that there is no appreciable side slip, and hence, the second equation may be ignored. What remains is known as Nomoto's equation. The two indicies, K and T, are related to the hydrodynamic coefficients by the following,

$$T_1 = \frac{(Y_{\dot{v}} - m)(N_r - mx_G U) + (N_{\dot{r}} - I_z)Y_v}{Y_v (N_r - mx_G U)_{N_v}(Y_r - mU)}$$

7

$$T_2 = \frac{-(Y_r - mx_G)N_v - (N_v - mx_G)(Y_r - mU)}{Y_v(N_r - mx_G U) - N_v(Y_r - mU)}$$

$$T_3 = \frac{(N_v - mx_G)Y_\delta - (Y_v - m)N_\delta}{N_v Y_\delta - Y_v N_\delta}$$

$$K = \frac{N_v Y_\delta - Y_v N_\delta}{Y_v(N_r - mx_G U) - N_v(Y_r - mU)}$$

where,
$$Y_{\dot{r}} = N_{\dot{v}} = 0.0$$

$$Y_r = m_1 - 1.5 s C_B$$

$$Y_v = -0.5\pi k + 1.4 s C_B$$

$$Y_{\dot{v}} = m - m_2$$

$$Y_\delta = -(1 + a_H)F_N$$

$$N_{\dot{v}} = -k$$

$$N_{\dot{r}} = I_{zz} - I$$

$$N_\delta = -(x_R + a_H x_H)F_N$$

$$N_r = -0.54 k + k^2$$

$$m_i = 2 s C_B(1 + \lambda_i), \quad i = 1,2 \quad \lambda_1 = k; \quad \lambda_2 = \frac{k}{s}(1 - \frac{s}{2});$$

8

$$I=(\frac{1}{8})sC_B(1+\lambda_6) \qquad \lambda_6=\frac{k}{s}(1-1.6s)$$

Nomoto's equation expresses the relationship between the ship's turning rate and the rudder angle through a second order transfer function,

$$\frac{r}{\delta}=\frac{K+KT_3s}{T_1T_2s^2+(T_1+T_2)s+1}$$

which can be simplified to a first order transfer function,

$$\frac{r}{\delta}=\frac{K}{Ts+1}$$

This equation in differential form is known as Nomoto's First Order Equation,

$$T\dot{r}+r=K\delta$$

where,

$$T=T_1+T_2+T_3$$

By using basic principles of ordinary differential equations, the solution for r, in terms of K and T, is given by,

$$r = K\delta(1-e^{-t/T})$$

Having developed these two models, nonlinear and liner, the two will now be compared to

see which will give a faster calculation time, and which is more accurate for graphical simulation.

III. MODEL ASSESSMENT

Having developed the nonlinear and linear (Nomoto's) models, the two were compared for speed of implementation and the relative accuracy for different inputs and geometric properties.

The principal dimensions of length, beam, and draft were varied independently and the models were also compared utilizing different rudder angle inputs.

In every instance of the comparison between these two models, the linear model proved to be approximately six times faster than the nonlinear model. This fact makes Nomoto's model ideally suited for visual simulation studies. Visual simulations may be carried out with minimal threat of reduced frame speed, due to calculation processing time.

A graph of the advance vs. transfer (i.e., a geographical x-y plot of the ship's path) is shown in Figure 2 for both linear and nonlinear models and for different rudder angles. Advance and transfer are shown in dimensionless form, with respect to the ship length. Rudder angle, indicated by d on the graphs, is in degrees. Solid curves correspond to the nonlinear simulation, while dotted curves correspond to Nomoto's first order model. It can be seen that the latter accurately depicts the ship's path for relatively large rudder angles. However, as the rudder angle is decreased the difference between linear and nonlinear simulations is likewise more pronounced. This deviation may be attributed to the increased side-slip velocities that are encountered during smaller rudder deflections and are neglected in Nomoto's model. This is explored in the next chapter.

The results for the yaw rate r are shown in Figure 3. Both yaw rate and time are shown in dimensionless quantities, with respect to ship speed and length. It seems that higher rudder angles result in slight overshoot in the yaw rate for the nonlinear model. This means that for high rudder angles, the yaw rate is basically described by a second order system, whose damping ratio becomes smaller.

The sensitivity of these results for small variations in the ship's draft is demonstrated by Figures 4 through 7. A plot of the advance vs. transfer for different values of the draft based on the nonlinear model is shown in Figure 4. It appears that small drafts correspond to more maneuverable ships with tighter turning circles. The same result can be drawn from the linear simulation results of Figure 5. From the yaw rate simulations of Figures 6 and 7, we can see that smaller drafts correspond to higher turning rates at steady state, as well as, at smaller time constants. The nonlinear simulations also suggest that a smaller draft results in smaller damping ratios, as evidenced by the overshoot in the yaw rate time history.

The sensitivity, with regards to ship beam, is demonstrated by Figures 8 throug 11. In general, it appears that the beam has very little effect on maneuverability. The nonlinear model suggests that maneuverability is increasing for increasing beam, although the linear model predicts the opposite. It also appears that the yaw rate damping ratio is decreased for decreasing values of the ship's beam.

The sensitivity, with regards to the ship length, is demonstrated by Figures 12 through 18. In general, both linear and nonlinear models suggest that maneuverability is increased with increasing length. This results in tighter turning circles, both in dimensional and dimensionless quantities.
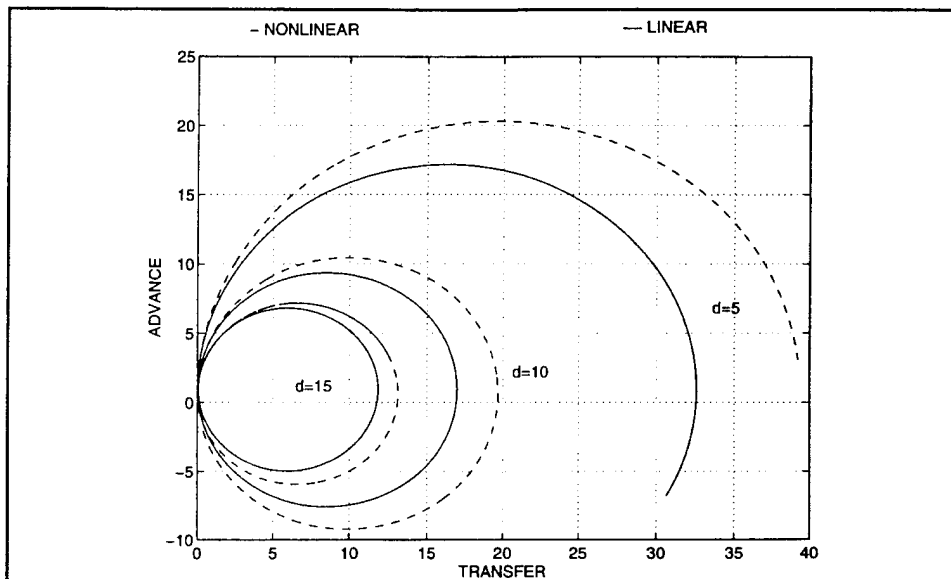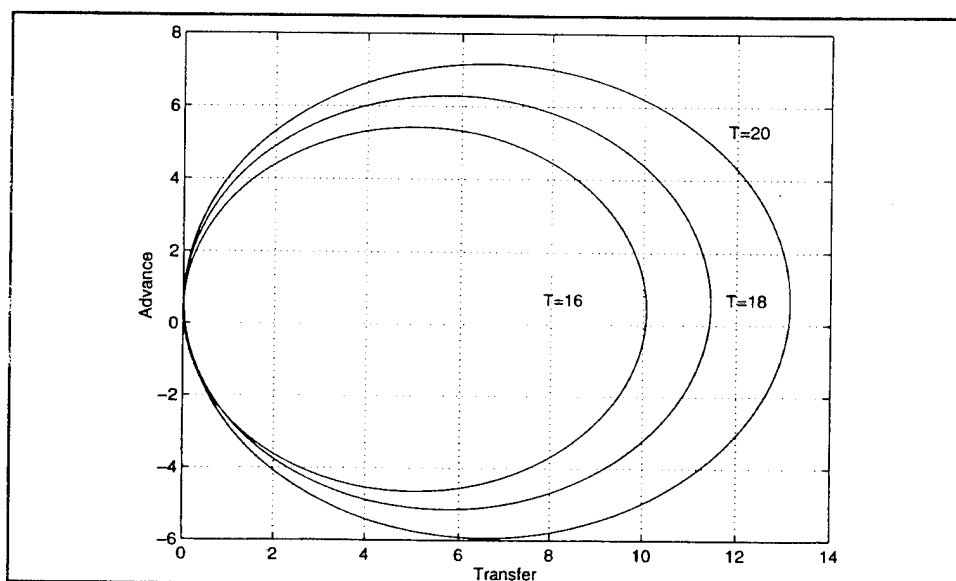
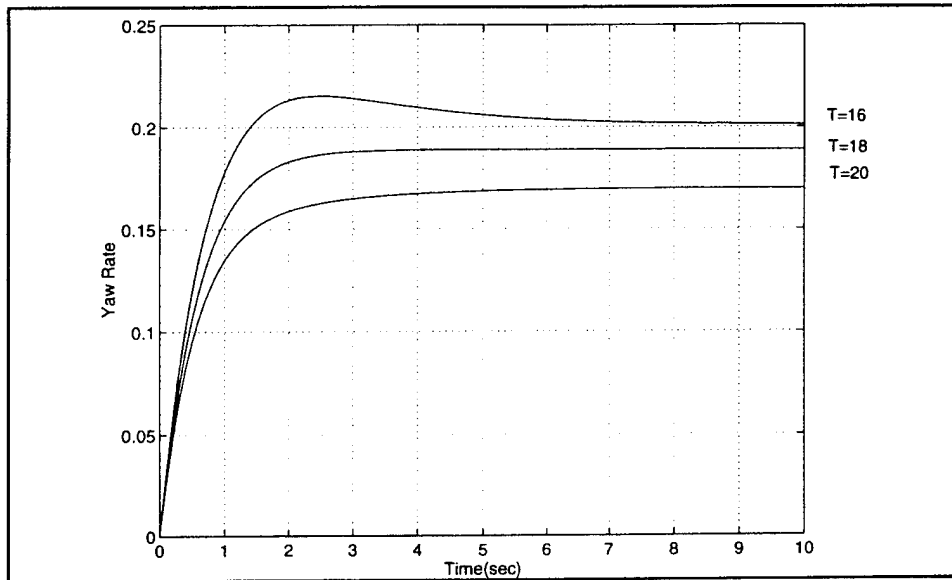**Figure 2** Rudder Angle comparison between Nonlinear Model and Nomoto's Model
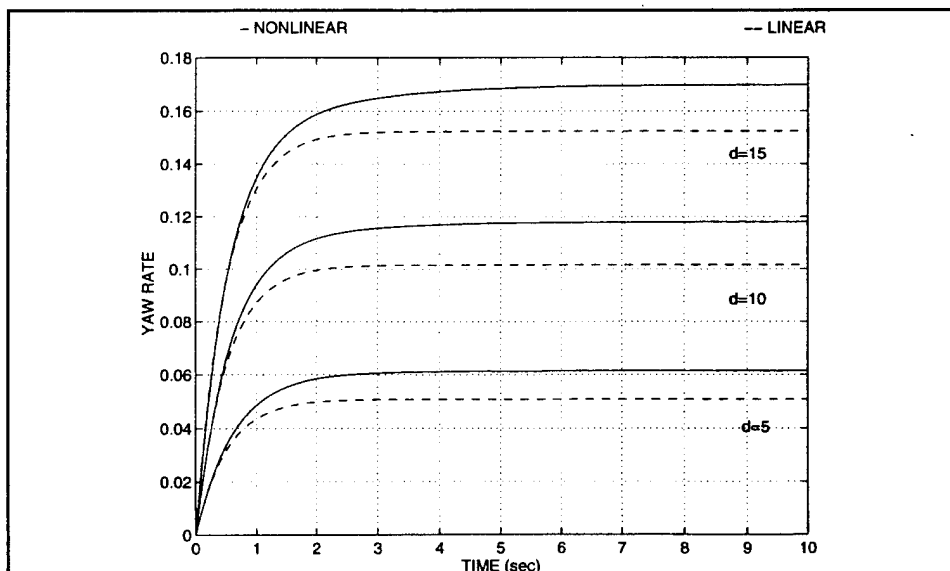
Figure 3 Yaw Rate comparison between Nonlinear Model and Nomoto's Model
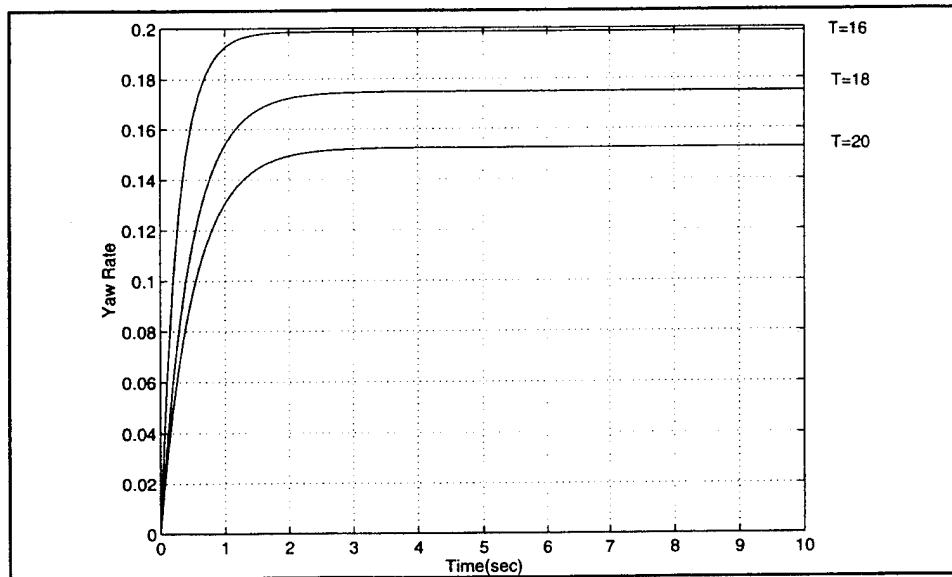
13
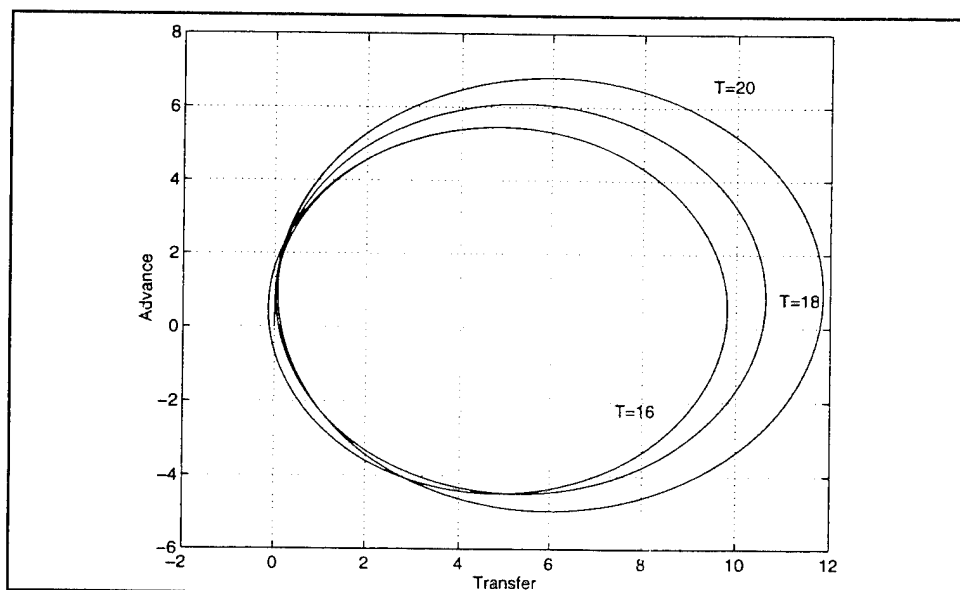
Figure 4 Advance vs. Transfer for Nonlinear Model at different drafts

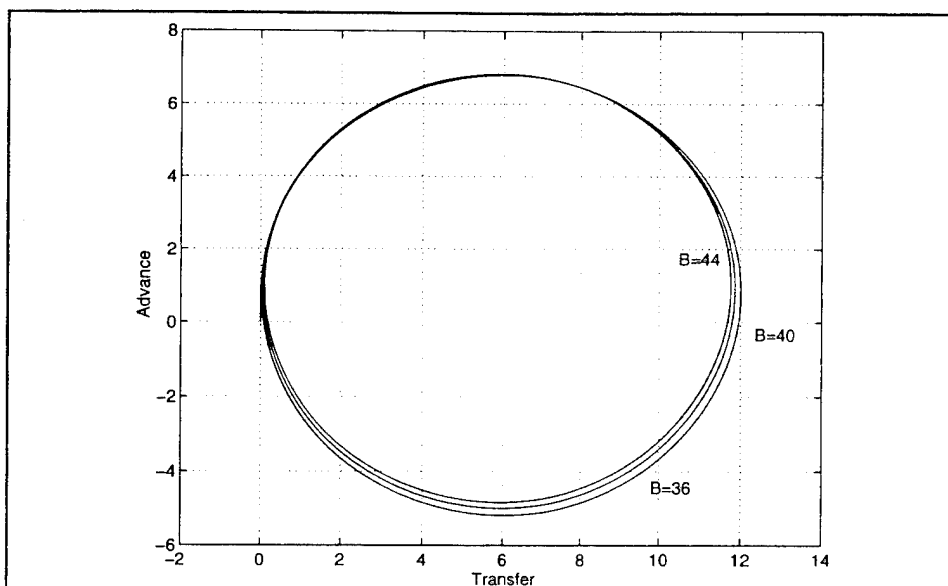**Figure 5** Advance vs. Transfer for Nomoto's Model at different drafts

14

Figure 6 Yaw Rate vs. Time for Nonlinear Model at varying drafts
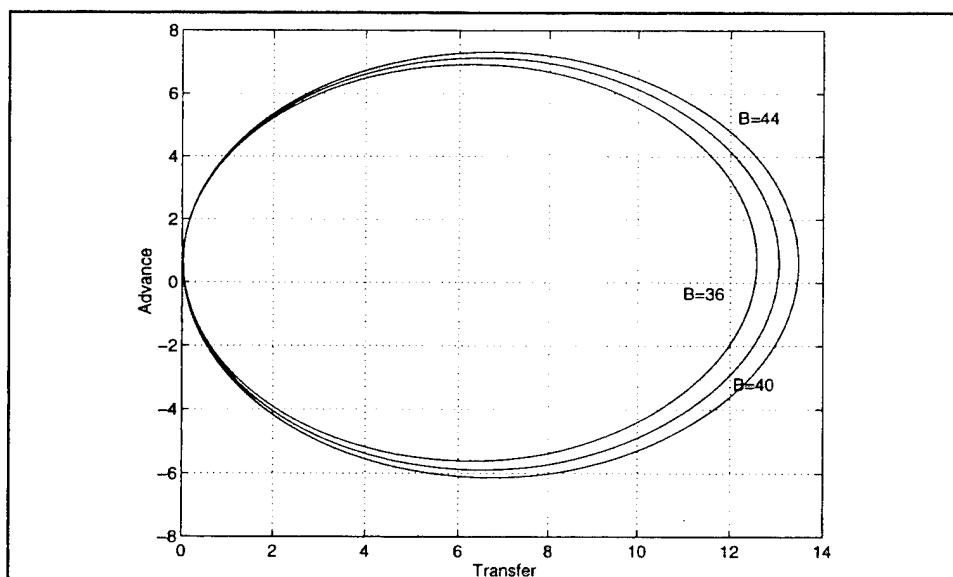

Figure 7 Yaw Rate vs. Time for Nomoto's Model at varying drafts

15

Figure 8 Advance vs. Transfer for Nonlinear Model at varying beams

Figure 9 Advance vs. Transfer for Nomoto's Model at varying beams

Figure 10 Yaw Rate vs. Time for Nonlinear Model at varying beams

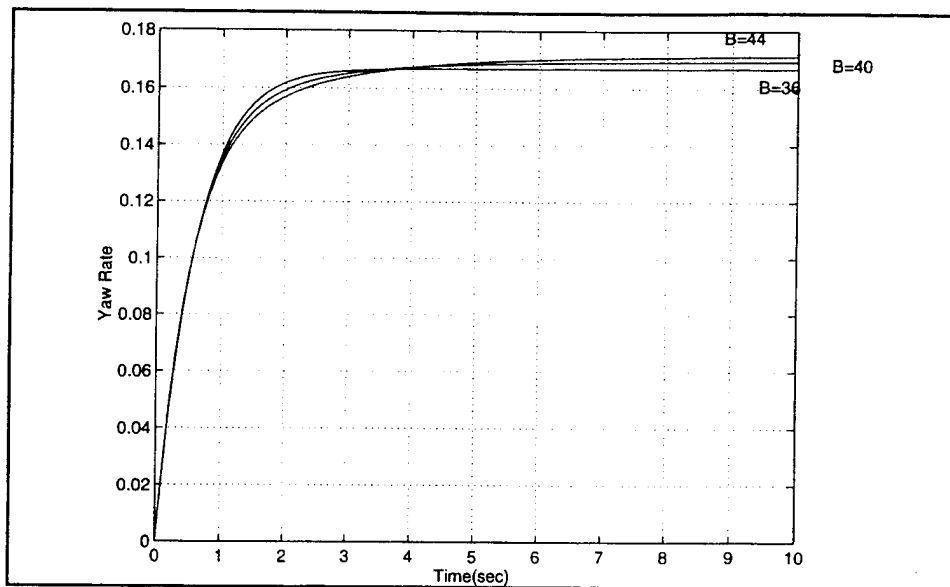**Figure 11** Yaw Rate vs. Time for Nomoto's Model at varying beams

17

Figure 12   Advance vs. Transfer for Nonlinear Model at varying lengths

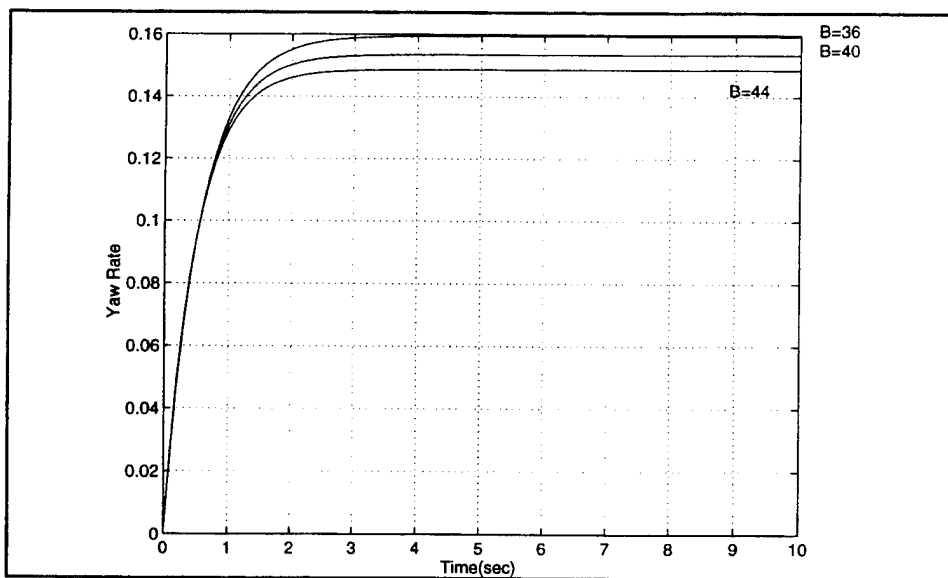**Figure 13** Dimensional Advance vs. Transfer for Nonlinear Model at varying lengths
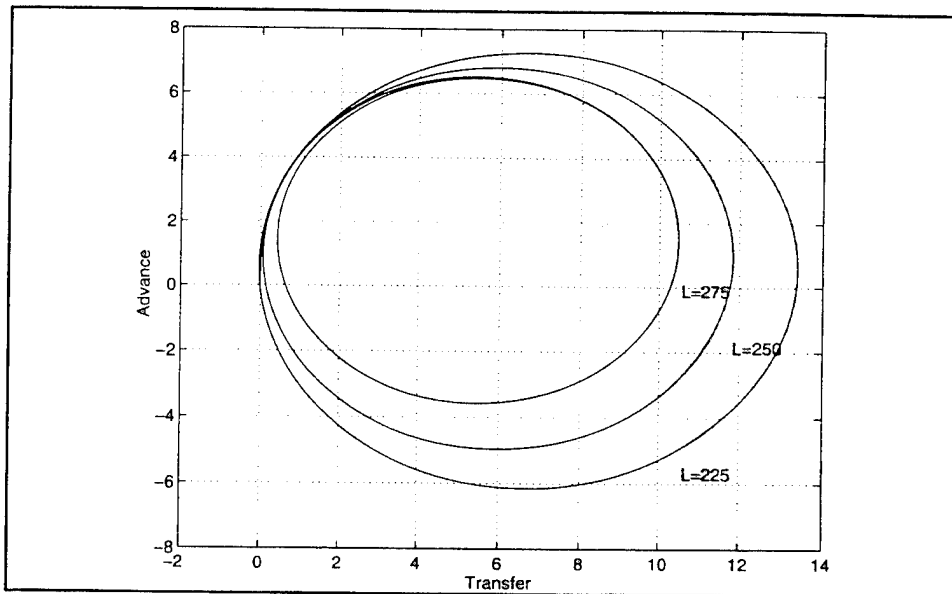
18

Figure 14 Advance vs. Transfer for Nomoto's Model at varying lengths

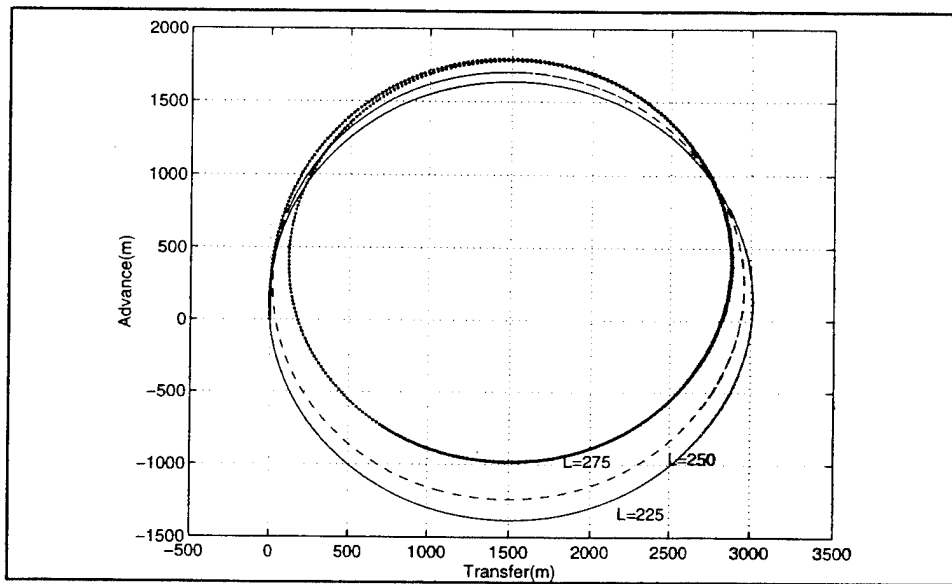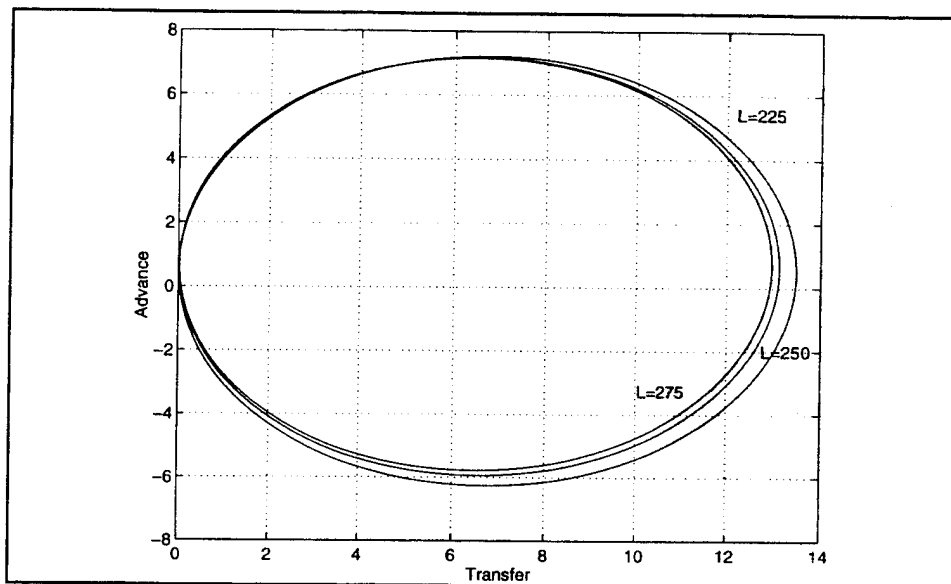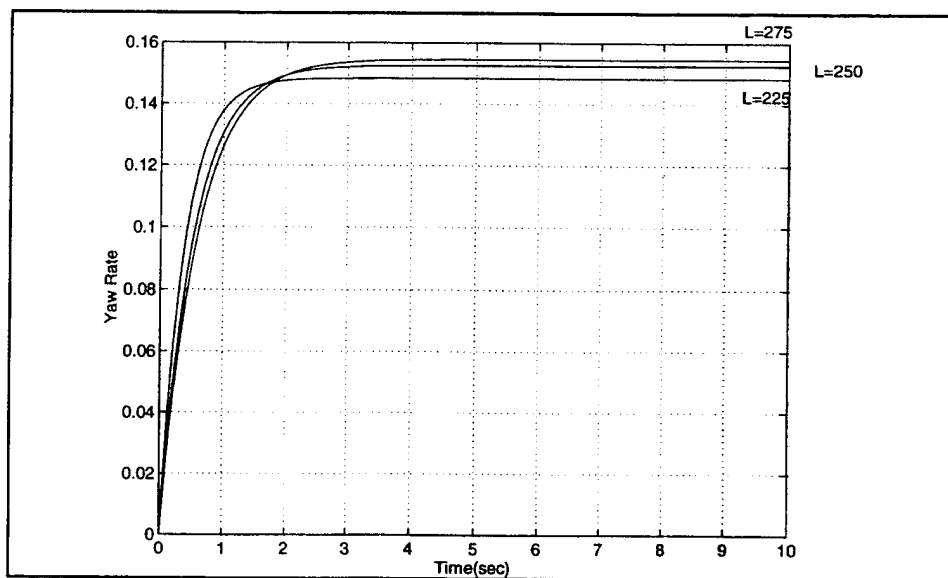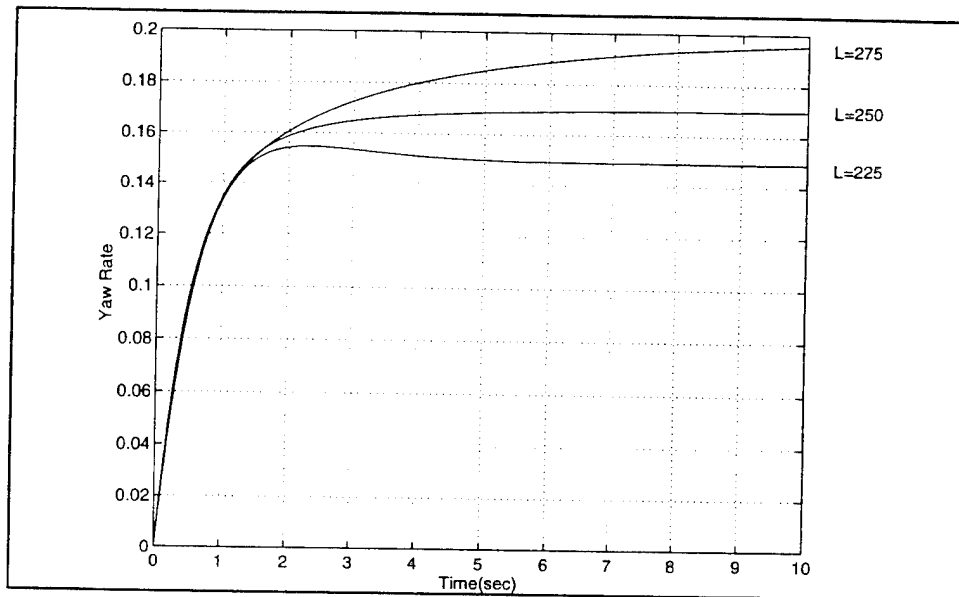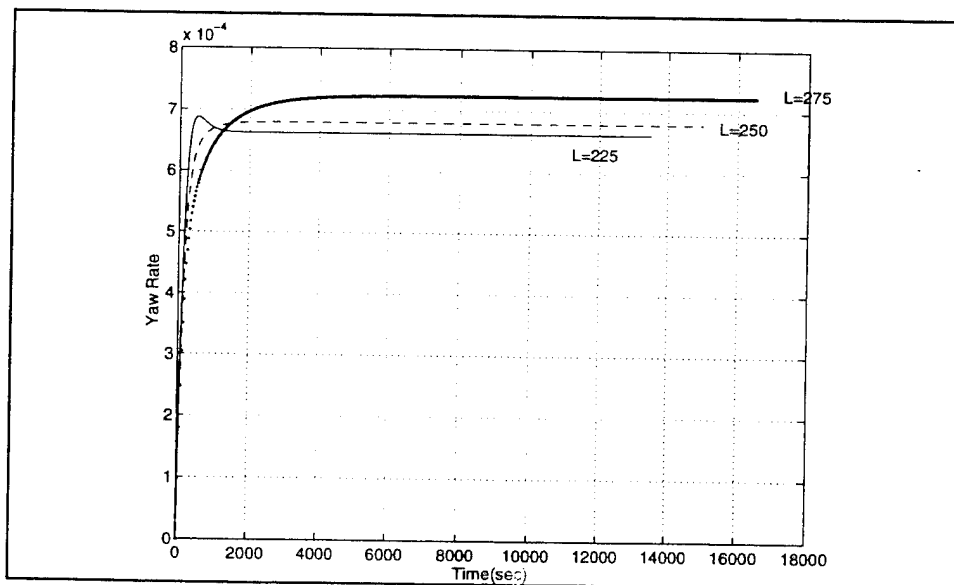**Figure 15** Yaw Rate vs. Time for Nomoto's Model at varying lengths

19

Figure 16 Yaw Rate vs. Time for Nonlinear Model at varying lengths

Figure 17 Dimensional Yaw Rate vs. Time for Nonlinear Model at varying lengths

20

IV. LINEAR MODEL VARIATION ASSESSMENT

In Chapter II, the assumption of negligible side slip velocity was made to obtain Nomoto's equation. If this assumption was not made, we would have the pair of decoupled second order equations from the linearized sway and yaw equations,

$$T_1 T_2 \ddot{v} + (T_1 + T_2) \dot{v} + v = K_v \delta + K_v T_4 \dot{\delta}$$

$$T_1 T_2 \ddot{r} + (T_1 + T_2) \dot{r} + r = K \delta + K T_3 \dot{\delta}$$

The relationship between the indicies, in the yaw rate second order equation and the hydrodynamic coefficients was shown in Chapter II. The indices of the side slip velocity second order equation are related to the hydrodynamic coefficients by the following,

$$K_v = \frac{(Y_r - m)N_\delta - (N_r - m x_G U)Y_\delta}{Y_v(N_r - m x_G U) - N_v(Y_r - mU)}$$

$$T_4 = \frac{(N_r - I_{zz})Y_\delta - (Y_r - m x_G U)N_\delta}{(N_r - m x_G U)Y_\delta - (Y_r - mU)N_\delta}$$

The second decoupled second order equation led to formulation of Nomoto's equation, and the first expresses the relationship between the side slip velocity and the rudder angle through a second order transfer function,

$$\frac{v}{\delta} = \frac{K_v + K_v T_4 s}{T_1 T_2 s^2 + (T_1 + T_2)s + 1}$$

which can be simplified to a first order transfer function,

$$\frac{v}{\delta} = \frac{K_v}{T_v s + 1}$$

21

This equation in differential form reduces to,

$$T_v \dot{v} + v = K_v \delta$$

where,

$$T_v = T_1 + T_2 - T_4$$

Once again, by using basic principles of ordinary differential equations the solution for the side slip velocity is,

$$v = K_v \delta (1 - e^{-\frac{t}{T_v}})$$

In Figure 18, a comparison is shown between Nomoto's model and a linear model containing the affects of side slip. The two graphs are almost identical, which leads to the conclusion that the original assumption of negligible side slip velocity was correct.

Now we will compare the nonlinear model with the side slip model. Figures 19 and 20 lead to the same conclusions as Figures 2 and 3, that relatively speaking, the nonlinear model is more accurate than the linear model. Figure 21 shows the comparison between the side slip velocity obtained in the nonlinear vs. the linear case. Once again, it is clear that the nonlinear model simulates the situation more accurately.

The side slip assessment leads to the conclusion that the difference between the linear and nonlinear models lies not with the side slip velocity, but with the yaw rate. It can be seen in Figure 22 that the difference in the error between the linear and nonlinear models is a function of the rudder angle.

By plotting the rudder angle vs. the steady-state yaw rate ratio (nonlinear over linear), we obtain a straight line as shown in Figure 23. By calculating the slope and intercept of this

line and applying it as a correction factor, we obtain a new relationship for Nomoto's equation,

$$T\dot{r} + r = (\alpha - \beta|\delta|)K\delta$$

By applying this "correction" factor, it can be seen in Figure 24 that we obtain a model that is more accurate than both Nomoto's model and the side slip model. On the average the corrected model is approximately 10% slower than Nomoto's model.

In Figure 25, it can be seen that the relative error in the yaw rate between the nonlinear model and Nomoto's model has been removed in the corrected model. By comparison, the conclusion that the corrected model is the most accurate of the models presented can be made. Due to the relative accuracy of the corrected model, it is better suited to simulate the turning rate while maintaining an acceptable frame speed during visual simulations.
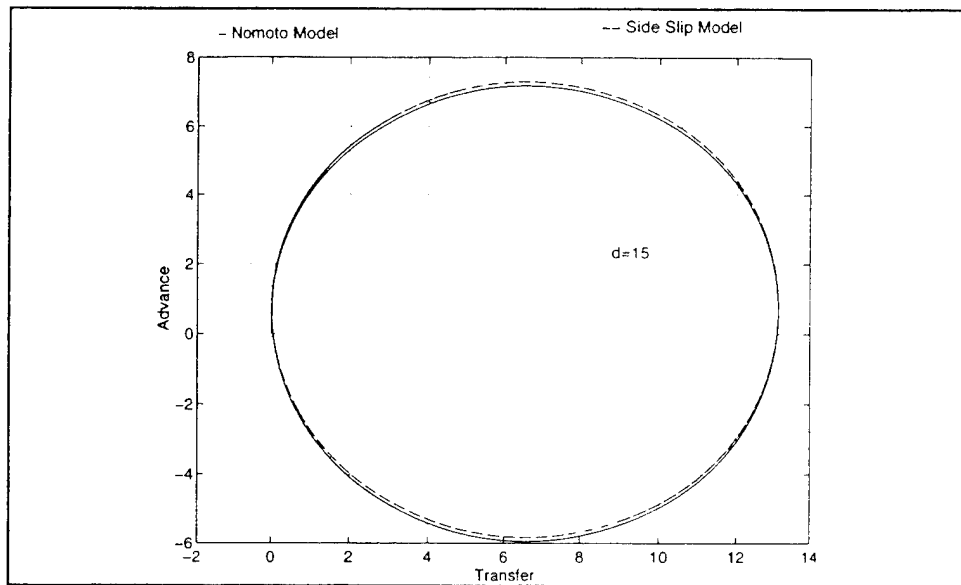
Figure 18 Advance vs. Transfer comparison between Nomoto's Model and Side Slip Model
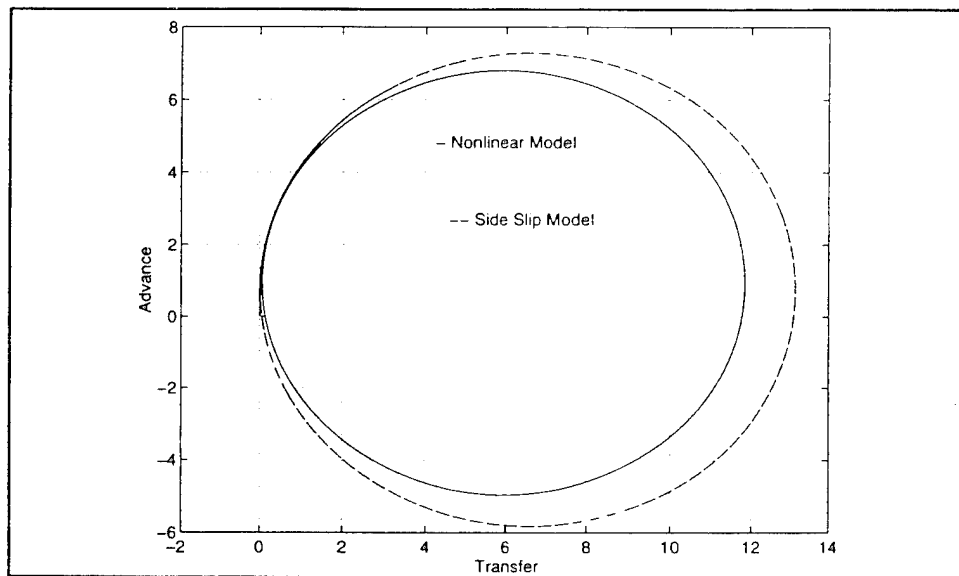
Figure 19 Advance vs.Transfer comparison between Nonlinear Model and Side Slip Model

24
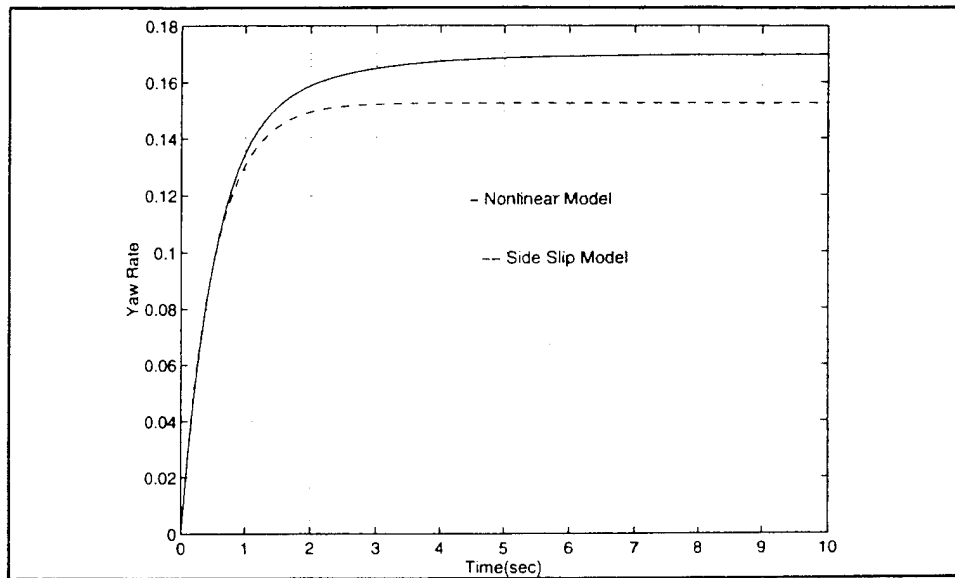
Figure 20 Yaw Rate vs. Time comparison between Nonlinear Model and Side Slip Model
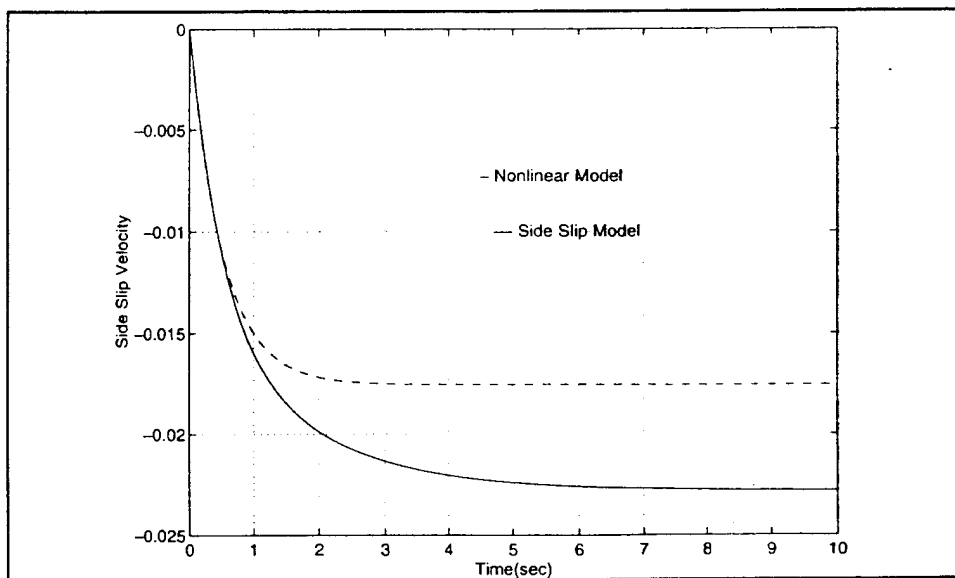
Figure 21 Side Slip Velocity comparison between Nonlinear Model and Side Slip Model

25
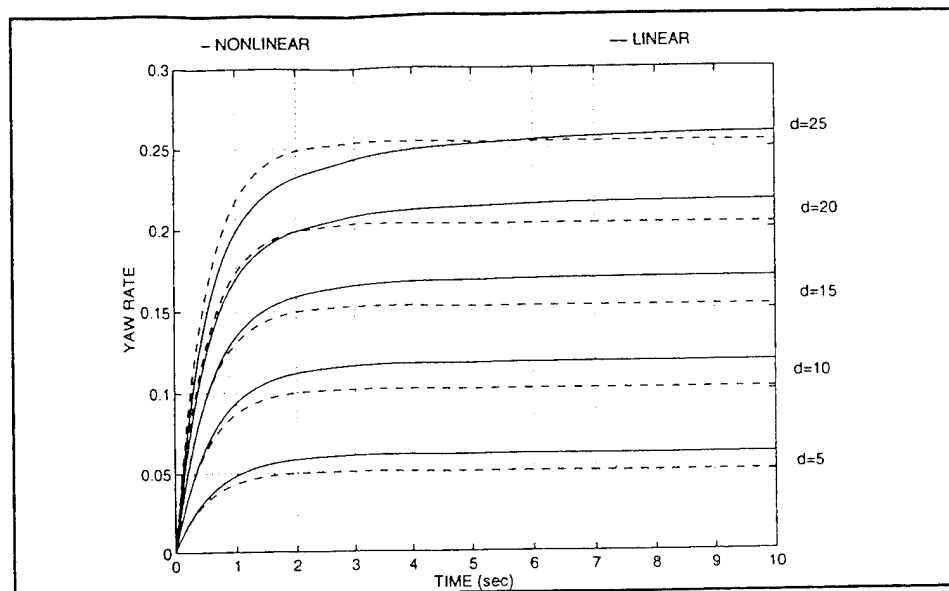
Figure 22 Yaw Rate vs. Time comparison between Nonlinear Model and Nomoto's Model at varying rudder angles
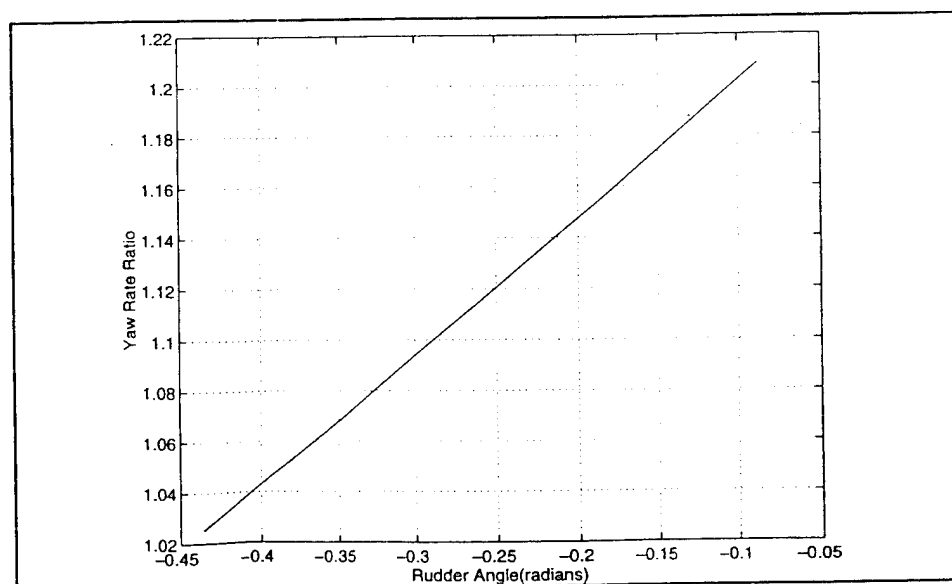
Figure 23 Yaw Rate Ratio vs. Rudder Angle plot used to obtain correction factor for Nomoto's Model

26
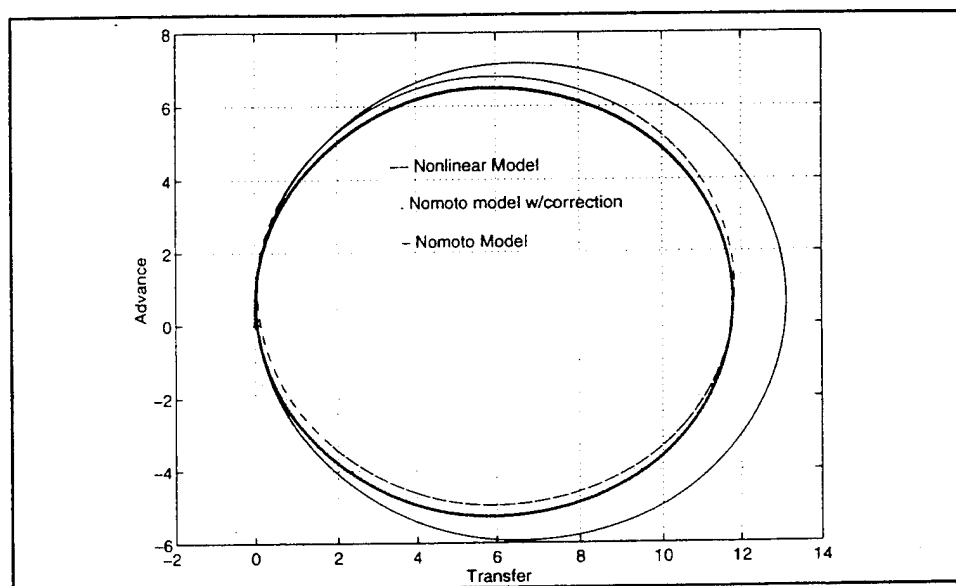
Figure 24 Advance vs. Transfer plot comparing Nonlinear, Nomoto, and corrected Nomoto Models
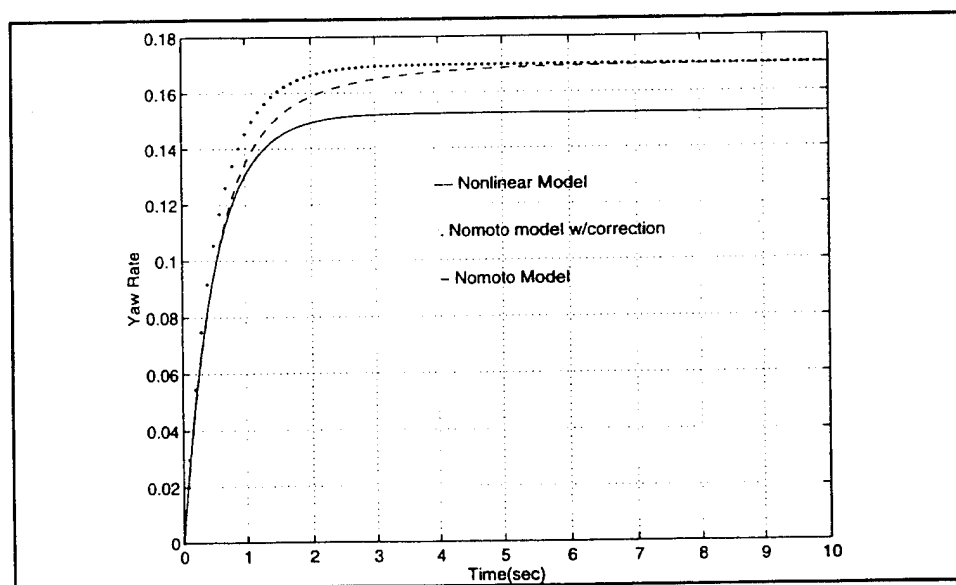
Figure 25 Yaw Rate vs. Time plot comparing Nonlinear, Nomoto, and corrected Nomoto Models

V. PARAMETRIC STUDY

During the preliminary ship design phase, it is often possible to introduce small changes in fundamental hull properties so that maneuverability is improved. Of course, such changes may only be instituted after taking due consideration of all aspects and requirements of the design problem.

In this Chapter, the maneuvering properties of a ship are explored by utilizing the nonlinear model described in the previous chapters, since it reflects reality better than the linear model. In order to establish a systematic series of runs, the ship's displacement was maintained constant. The dispalcement is usually determined by payload considerations and it is unlikely that a designer would have the freedom to change it based on maneuvering requirements alone.

Figures 26 and 27 show results that are obtained by keeping both the displacement and the beam constant. The length and draft are then changed within plus/minus 5% of their nominal values. It can be seen that the longer and shallower hull form has superior maneuvering characteristics compared to shorter and deeper draft ships.

Figures 28 and 29 show results that are obtained by keeping both the displacement and the length constant. The beam and draft are then changed within plus/minus 5% of their nominal values. It can be seen that wide, shallow hull forms have superior maneuvering characteristics compared to narrow and deeper draft ships.

Figures 30 and 31 show results that are obtained by keeping both the displacement and the draft constant. The length and beam are then changed within plus/minus 5% of their nominal values. It can be seen that the long and narrow hull forms have superior maneuvering characteristics compared to shorter and wider draft ships.

Maneuvering performance is increased by:

- a longer length
- less draft
- a narrower beam for constant draft
- a wider beam for constant length

Therefore, beam does not have a consistent trend and since it is usually set by static stability considerations, it should not be altered based on maneuvering alone. The length is the most costly dimension to increase. Not only are material cost increased, but dry dock size, and shipbuilding considerations must also come into play. The draft on the othe hand will have it's own set of considerations such as harbor and canal restrictions.

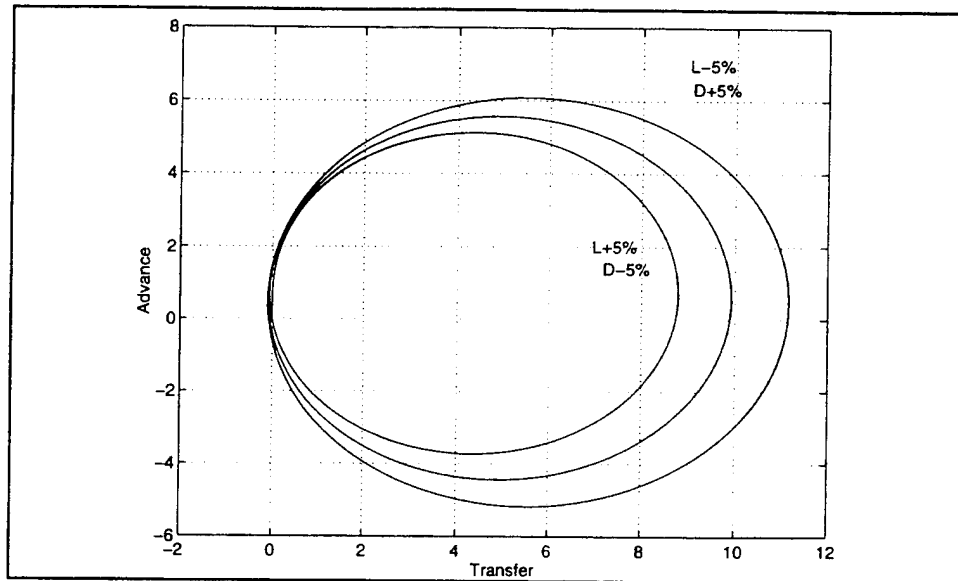**Figure 26** Advance vs. Transfer comparison with constant beam
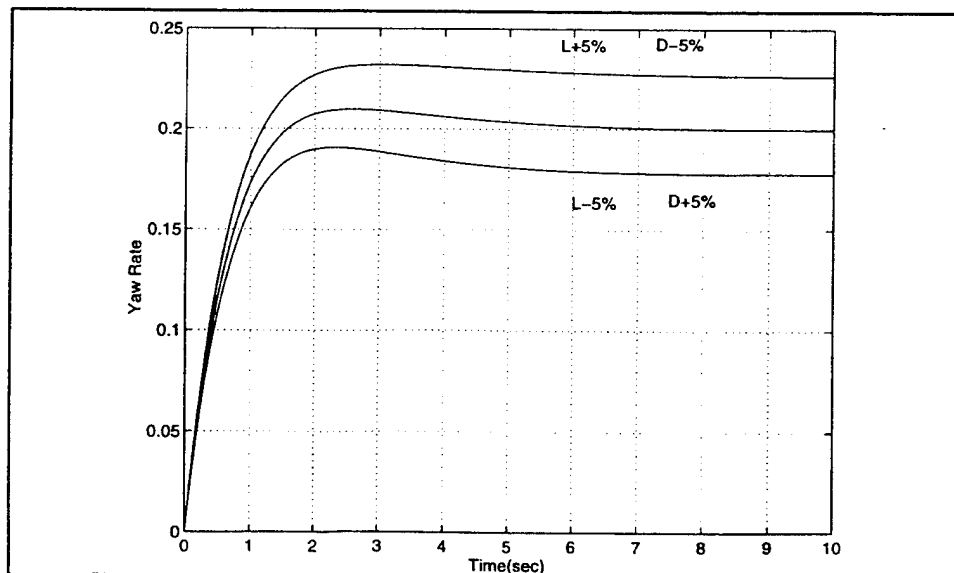

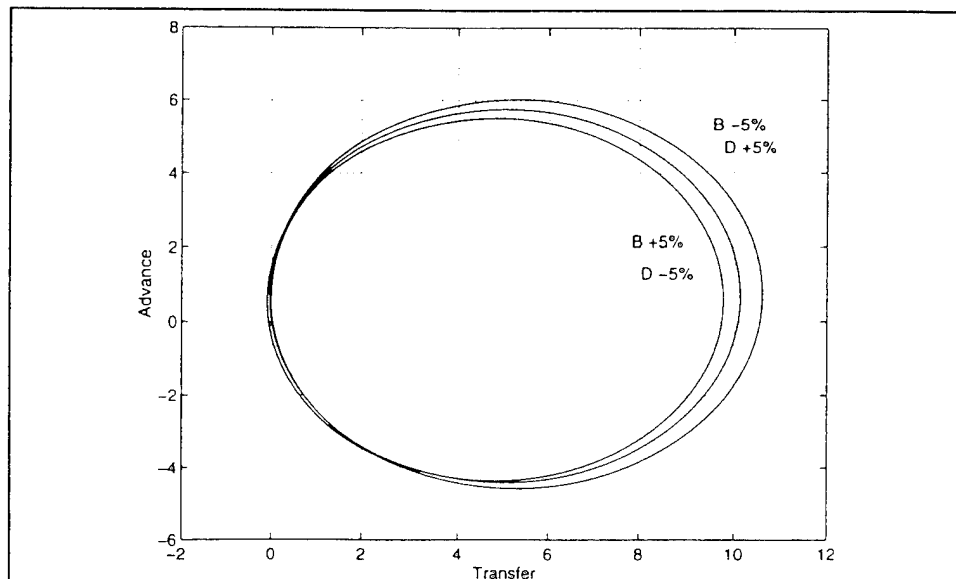**Figure 27** Yaw Rate vs. Time comparison with constant beam

31

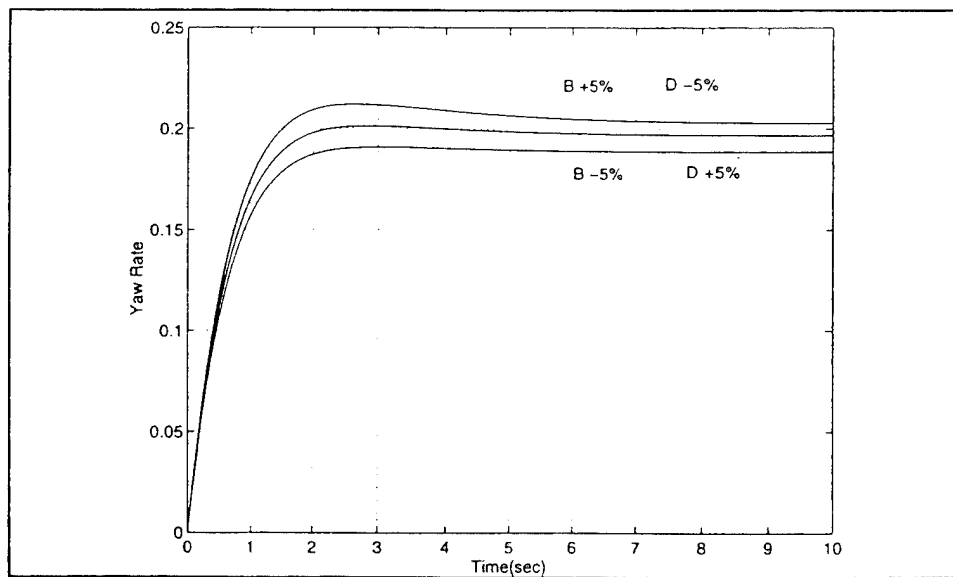**Figure 28** Advance vs. Transfer comparison with constant length

Figure 29 Yaw Rate vs. Time comparison with constant length

32
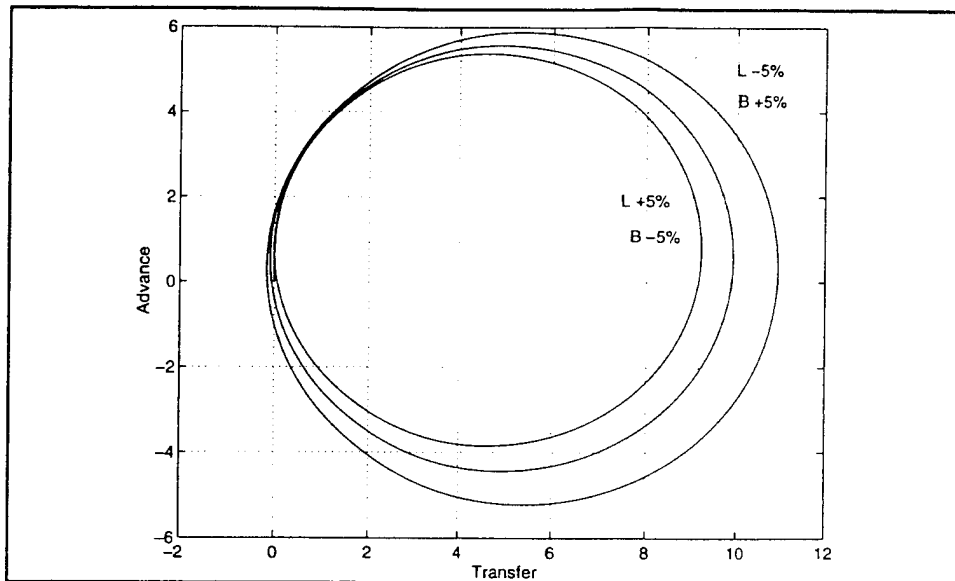
Figure 30 Advance vs. Transfer comparison with constant draft
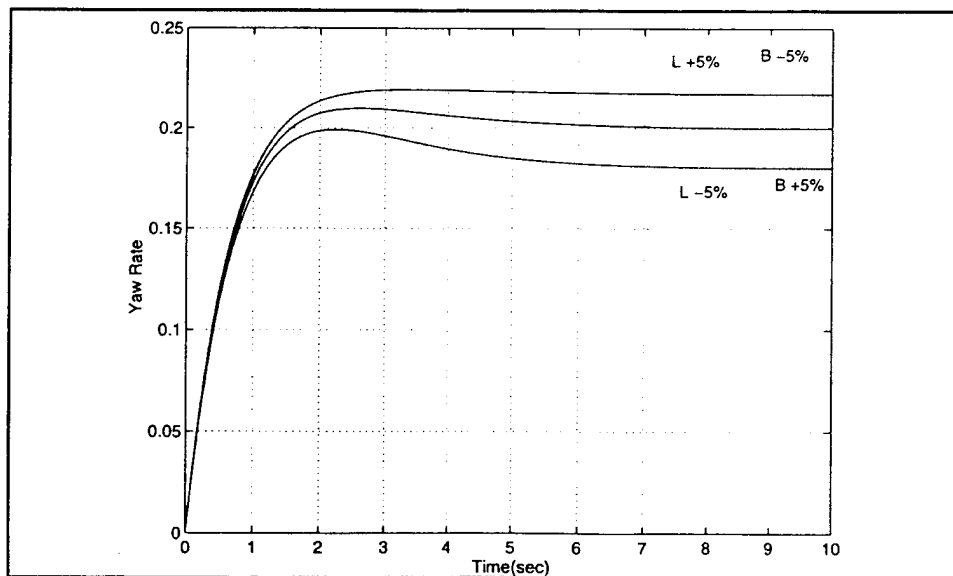
Figure 31 Yaw Rate vs. Time comparison with constant draft

VI. CONCLUSIONS

In this thesis two maneuvering models were developed and compared. A nonlinear model based on ship geometric and mass properties was developed from [Ref. 1]. The second, linear, model was developed by linearizing the sway and yaw equations of the nonlinear model, as done in [Ref. 3]. The models were compared for speed of implementation and the relative accuracy for different inputs and geometric properties. It was concluded that though the linear model was approximately six times faster than the nonlinear model, it was not accurate enough.

At this point a variation was made to the linear model by adding the effects of the side slip velocity to possibly explain the difference in the accuracy. Upon further inspection, it was determined that the difference in accuracy did not lie with the side slip velocity, but with the difference in the yaw rates.

By plotting the rudder angle vs. the steady-state yaw rate ratio, a correction factor was obtained and applied to the linear model ;causing the steady-state error between the yaw rates of the linear and nonlinear models to be removed altogether. This "corrected" linear model also proved to be relatively more accurate than either the original linear model and the nonlinear model. Though this model is 10% slower than the original linear model, it is still much faster than the nonlinear model.

A series of parametric studies was also performed on the nonlinear model in order to evaluate the sensitivity of fundamental maneuvering properties in terms of basic ship geometric quantities. It was concluded that maneuvering performance is increased by a longer length or by less draft. The beam did not show a consistent trend, and is usually set by static stability considerations and probably not alterable for maneuvering alone.

For further work, it is recommended that these models be incorporated into the Computer Science Department battlespace simulation system, NPSNET. Initially this system was geared towards ground forces and land based conflicts, but recently a naval component has been added in an attempt of attaining a more realistic joint services simulator. The models should be checked for accuracy, realism, and speed of implementation. Once a baseline is obtained, improvements in the best model for visual simulation can be made.

APPENDIX. MATLAB CODE

Nondimensional quantities, denoted by primes, are defined as follows:

$m' = m/(0.5\rho L^2 d)$

$m_x' = m_x/(0.5\rho L^2 d)$

$m_y' = m_y/(0.5\rho L^2 d)$

$I_{zz}' = I_{zz}/(0.5\rho L^4 d)$

$i_{zz}' = i_{zz}/(0.5\rho L^4 d)$

$X' = X/(0.5\rho L d U^2)$

$Y' = Y/(0.5\rho L d U^2)$

$N' = N/(0.5\rho L^2 d U^2)$

$r' = r L/U$

```
% COMPARISON OF LINEAR AND NONLINEAR MODELS
% ON SAME GRAPH(including Nomoto correction & side slip model)
%
% Define parameters of the simulation (Metric units)
%
%
time = 90.0;                                % Final time of simulation
dt = .1;                                    % Sample time of difference eqns
Iz = 3257400.;                              % Moment of inertia
L = 250.0;                                  % ship's length
RHO = 1025;                                 % Density of salt water
XG = 10.0;                                  % Center of gravity
Mass = 147241915.0;                         % Ship mass
m = Mass/(0.5*RHO*L^3);                     % Dimensionless ship mass
Izz = Iz/(0.5*RHO*L^5);                     % Dimensionless moment of inertia
Xg = XG/L;                                  % Dimensionless center of gravity
d = -0.2618;                                % rudder angle
B = 40.77;                                  % ship's breath(twice the beam)
D = 20.00;                                  % ship's draft
s = B/L;                                    % slenderness ratio
V = Mass/RHO;                               % ship's displacement
Cb = V/(L*D*B);                             % block coeff
k = 2*D/L;                                  % hull aspect ratio
Kr = 1.7;                                   % rudders aspect ratio
AR = 74.0;                                  % rudder area
Dp = 8.5;                                   % propeller diameter
P = 0.8*Dp;
n = 1000;                                   % propeller revolution (rps)
Ctp = 1.0;
aH = 0.633*Cb - 0.153;
eps = -156.2*(Cb*B/L)^2 + 41.6*(Cb*B/L) - 1.76;
wp = 0.23 + 1.4*(Cb - 0.5)^2;
tp = 0.6*wp;                                % thrust deduction coefficient
wr = 1 - (eps*(1-wp));
K = 0.6*(1-wp)/(1-wr);
tr = 0.28*Cb + 0.55;
eta = Dp/(sqrt(AR*Kr));
Cn = (6.13*Kr)/(Kr + 2.25);
lambda6 = (k/s)*(1-1.6*s);
I = (1/8)*s*Cb*(1+lambda6);
lambda2 = (k/s)*(1-s/2);
m2 = 2*s*Cb*(1+lambda2);
lambda1 = k;
m1 = 2*s*Cb*(1+lambda1);
PI = 3.14;
xR = -0.5;
xH = -0.5;
m1 = 2*s*Cb*(1+lambda1);
gamma = -22.2*(Cb*B/L)^2 + 0.02*(Cb*B/L) + 0.68;
U = 1.0;
UR = U;
%
% LINEAR MODELS
%
beta = .25;                                 % drift angle
Fn= -(AR/(L*D))*Cn*UR^2*cos(- gamma*beta); % Force acting on rudder
%
% Define hydrodynamic coefficients
%
Yv1 = -0.5*PI*k + 1.4*s*Cb;
Nv1 = -k;
Yr1 = m1 - 1.5*s*Cb;
Yd1 = -(1+aH)*Fn;
Nr1 = -0.54*k + k^2;
Nd1 = -(xR + aH*xH)*Fn;
Nr1dot = Izz-I;
Yv1dot = m-m2;
Yr1dot = 0.0;
Nv1dot = 0.0;
%
% Define constants of Nomoto's first order equation
%
K = (Nv1*Yd1 - Yv1*Nd1)/[Yv1*(Nr1-m*Xg) - Nv1*(Yr1-m)];
Kv = -[(Nr1-m*Xg)*Yd1 - (Yr1-m)*Nd1]/[Yv1*(Nr1-m*Xg) - Nv1*(Yr1-m)];
T1 = [(Yv1dot-m)*(Nr1-m*Xg) + Yv1*(Nr1dot-Izz)]/[Yv1*(Nr1-m*Xg) - Nv1*(Yr1-m)];
T2 = [(Nv1dot-m*Xg)*(Yr1-m) - Nv1*(Yr1dot-m*Xg)]/[Yv1*(Nr1-m*Xg) - Nv1*(Yr1-m)];
T3 = [Yd1*(Nv1dot-m*Xg) - Nd1*(Yv1dot-m)]/[Nv1*Yd1 - Yv1*Nd1];
```

38

```
T4 = [(Nr1dot - Izz)*Yd1 - (Yr1dot - m*Xg)*Nd1]/[(Nr1-m*Xg)*Yd1 - (Yr1-m)*Nd1];
T = T1+T2-T3;
Tv = T1+T2-T4;
%
% Define storage vectors for Nomoto's Model
%
kmax1 = (time/dt)+ 1;                      % Number of data points
r1 = zeros(1,kmax1);                       % Initialize angular velocity vector
r1dot = zeros(1,kmax1);                    % Initialize angular acceleration vector
psi1 = zeros(1,kmax1);                     % Initialize heading angle vector
psi1dot = zeros(1,kmax1);                  % Initialize Yaw rate vector
XL = zeros(1,kmax1);                       % Initialize X position vector(including side slip)
XLdot = zeros(1,kmax1);                    % Initialize forward velocity vector(including side sli
p)
YL = zeros(1,kmax1);                       % Initialize Y position vector(including side slip)
YLdot = zeros(1,kmax1);                    % Initialize side slip velocity vector(including side s
lip)
%
% Define storage vectors for Side Slip Model
%
v2 = zeros(1,kmax1);                       % Initialize side slip veloctiy vector
v2dot = zeros(1,kmax1);                    % Initialize side slip acceleration vector
X2 = zeros(1,kmax1);                       % Initialize X position vector(including side slip)
X2dot = zeros(1,kmax1);                    % Initialize forward velocity vector(including side sli
p)
Y2 = zeros(1,kmax1);                       % Initialize Y position vector(including side slip)
Y2dot = zeros(1,kmax1);                    % Initialize side slip velocity vector(including side s
lip)
%
% Define storage vectors for Nomoto's Model w/correction factor
%
r3 = zeros(1,kmax1);                       % Initialize angular velocity vector
r3dot = zeros(1,kmax1);                    % Initialize angular acceleration vector
psi3 = zeros(1,kmax1);                     % Initialize heading angle vector
psi3dot = zeros(1,kmax1);                  % Initialize Yaw rate vector
X3 = zeros(1,kmax1);                       % Initialize X position vector(including side slip)
X3dot = zeros(1,kmax1);                    % Initialize forward velocity vector(including side sli
p)
Y3 = zeros(1,kmax1);                       % Initialize Y position vector(including side slip)
Y3dot = zeros(1,kmax1);                    % Initialize side slip velocity vector(including side s
lip)
Time1 = zeros(1,kmax1);                    % Initialize time vector
%
for i = 1:kmax1-1;
%
% Calculation loop for Nomoto's Model
%
r1dot(i) = (K*d - r1(i))/T;
r1(i+1)= r1(i) + r1dot(i)*dt;
psi1dot(i) = r1(i);
psi1(i+1)= psi1(i) + psi1dot(i)*dt;
XLdot(i) = cos(psi1(i));
XL(i+1) = XL(i) + XLdot(i)*dt;
YLdot(i) = sin(psi1(i));
YL(i+1) = YL(i) + YLdot(i)*dt;
%
% Calculation loop for Side Slip Model
%
v2dot(i) = (Kv*d - v2(i))/Tv;
v2(i+1) = v2(i) + v2dot(i)*dt;
X2dot(i) = cos(psi1(i))- v2(i)*sin(psi1(i));
X2(i+1) = X2(i) + X2dot(i)*dt;
Y2dot(i) = sin(psi1(i))+ v2(i)*cos(psi1(i));
Y2(i+1) = Y2(i) + Y2dot(i)*dt;
%
% Calculation loop for Nomoto's Model w/correction factor
%
R=0.5424*d+1.2560;
r3dot(i) = (R*K*d - r3(i))/T;
r3(i+1)= r3(i) + r3dot(i)*dt;
psi3dot(i) = r3(i);
psi3(i+1)= psi3(i) + psi3dot(i)*dt;
X3dot(i) = cos(psi3(i));
X3(i+1) = X3(i) + X3dot(i)*dt;
Y3dot(i) = sin(psi3(i));
Y3(i+1) = Y3(i) + Y3dot(i)*dt;
Time1(i+1) = Time1(i) + dt;
```

```
%
end
%
% NONLINEAR MODEL
%
% Define hydrodynamic coefficients
%
Yb = -0.5*PI*k + 1.4*s*Cb;
YR = m1 - 1.5*s*Cb;
Ybb = 1.25*(k/s)*(1-Cb) + 0.5;
Yrr = 0.17*(k/s)*Cb - 0.07;
Ybrr = 2.97*(k/s)*(1-Cb);
Ybbr = 0.75*(k/s)*Cb - 0.65;
Nb = -k;
NR = -0.54*k + k^2;
Nbb = -0.48*(k/s)*(1-Cb) + .066;
Nrr = 0.5*s*Cb - .09;
Nbrr = -0.25*(k/s)*Cb + 0.05;
Nbbr = -57.5*(s*Cb)^2 + 18.4*s*Cb - 1.6;
Xudot = m-m1;
Nrdot = Izz-I;
Yvdot = m-m2;
Yrdot = 0.0;
Nvdot = 0.0;
Xbr = 0.0;
Xuu = 0.0;
U = 1.0;
UR = U;                                    % effective rudder inflow speed
%
% Define storage vectors in advance to optimize performance
%
kmax = (time/dt)+1;                        % Number of data points
v = zeros(1,kmax);                         % Initialize side slip veloctiy vector
r = zeros(1,kmax);                         % Initialize angular velocity vector
rdot = zeros(1,kmax);                      % Initialize angular acceleration vector
b = zeros(1,kmax);                         % Initialize drift angle vector
bdot = zeros(1,kmax);                      % Initialize drift acceleration vector
X = zeros(1,kmax);                         % Initialize X position vector
Xdot = zeros(1,kmax);                      % Initialize forward velocity vector
Y = zeros(1,kmax);                         % Initialize Y position vector
Ydot = zeros(1,kmax);                      % Initialize side slip velocity vector
psi = zeros(1,kmax);                       % Initialize heading angle vector
psidot = zeros(1,kmax);                    % Initialize yaw rate vector
Time = zeros(1,kmax);                      % Initialize time vector
%
% Define nonlinear equations [calculation loop]
%
for i = 1:kmax-1;
Fn = -(AR/(L*D))*Cn*UR^2*sin(d - gamma*(b(i)-(2*xR*r(i)))); % Force acting on rudde
Xr = -(1-tr)*Fn*sin(d);
Yr = -(1+aH)*Fn*cos(d);
Nr = -(xR + aH*xH)*Fn*cos(d);
%
Xh = Xbr*r(i)*sin(b(i)) + Xuu *(cos(b(i)))^2;
Yh = b(i)*Yb + r(i)*YR + r(i)*(abs(r(i)))*Yrr + b(i)*(abs(b(i)))*Ybb + (b(i))^2*r(i)*Ybbr + b(i
)*(r(i))^2*Ybrr;
Nh = b(i)*Nb + r(i)*NR + r(i)*(abs(r(i)))*Nrr + b(i)*(abs(b(i)))*Nbb + (b(i))^2*r(i)*Nbbr + b(i
)*(r(i))^2*Nbrr;
%
Yp = 0.0;
Np = 0.0;
Jp = (U*cos(b(i))*(1-wp))/(n*Dp);
c1=0.52;
c2=-0.4861;
c3=0.01212;
Kt = c1 + c2*Jp + c3*Jp^2;
Xp = (Ctp*(1-tp)*n^2*Dp^4*Kt)/(0.5*L*D*U^2);
%
X1 = Xh + Xr + Xp;
Y1 = Yh + Yr + Yp;
N1 = Nh + Nr + Np;
%
f1 = (m-Yvdot)*(Izz-Nrdot) - (Nvdot-m*Xg)*(Yrdot-m*Xg);
f2 = Y1- m*r(i);
f3 = N1- m*Xg*r(i);
%
rdot(i) = [(m-Yvdot)*f3 + (Nvdot-m*Xg)*f2]/f1;
```

```
r(i+1) = r(i) + rdot(i)*dt;
bdot(i) = [(Izz-Nrdot)*f2 + (Yrdot-m*Xg)*f3]/f1;
b(i+1)= b(i) + bdot(i)*dt;
v(i) = U*tan(b(i));
psidot(i) = r(i);
psi(i+1) = psi(i) + psidot(i)*dt;
Xdot(i) = cos(psi(i)) - v(i)*sin(psi(i));
X(i+1) = X(i) + Xdot(i)*dt;
Ydot(i) = sin(psi(i)) + v(i)*cos(psi(i));
Y(i+1) = Y(i) + Ydot(i)*dt;
Time(i+1) = Time(i) + dt;
end
%
% Plot results
%
figure(1)
plot(Y,X,'--',YL,XL,'-',Y3,X3,'.'),grid;
xlabel('Transfer'),ylabel('Advance');
gtext('-- Nonlinear Model');
gtext('. Nomoto model w/correction');
gtext('- Nomoto Model');
%
figure(2)
plot(Time(1:101),r(1:101),'--',Time1(1:101),r1(1:101),'-',Time1(1:101),r3(1:101),'.'),grid;
xlabel('Time(sec)'),ylabel('Yaw Rate')
gtext('-- Nonlinear Model');
gtext('. Nomoto model w/correction');
gtext('- Nomoto Model');
%
```

LIST OF REFERENCES

1.   YAVIN, ZILMAN, AND MILOH, *A Feasibility Study of Ship Maneuverability in the Vicinity of an Obstacle: A Stochastic Control Approach.*

2.   KATSUTO, KIJIMA ET. AL., *On a Numerical Simulation for Predicting of Ship Maneuvering Performance,* Proceedings 19th International Towing Tanks Conference, Vol. 2, 1990.

3.   PAPOULIAS, F. A., *Dynamics of Marine Vehicles: Informal Lecture Notes,* Department of Mechanical Engineering, Naval Postgraduate School, 1993.

4.   INOUE, S., HIRANO, M., KIJIMA, K. AND TAKASHINA, J., *A Practical Calculation Method of Ship Maneuvering Motion,* International Shipbuild, Progr., 28, No. 325, pp. 207-222, 1981.

5.   INOUE, S., HIRANO, M., KIJIMA, K., *Hydrodynamic Derivatives on Ship Maneuvering,* International Shipbuild, Progr., Vol. 28, No. 321, pp. 112-125, 1981.

INITIAL DISTRIBUTION LIST

No. Copies

1. Defense Technical Information Center   2
   8725 John J. Kingman Rd., STE 0944
   Ft. Belvoir, Virginia 22060-6218

2. Library, Code 13   2
   Naval Postgraduate School
   Monterey, California 93943-5101

3. Chairman, Code ME   1
   Department of Mechanical Engineering
   Naval Postgraduate School
   Monterey, California 93943-5000

4. Professor Fotis A. Papoulias, Code ME/PA   6
   Department of Mechanical Engineering
   Naval Postgraduate School
   Monterey, California 93943-5100

5. Naval Engineering Curricular Office, Code 34   1
   Naval Postgraduate School
   Monterey, California 93943-5100

6. LT Patrick B. LaFontant   2
   91-31 Lamont ave, apt 5M
   Elmhurst, N.Y. 11373